

UNIVERSITY OF HAMBURG

MASTER'S THESIS

Automated Analysis of Meso-Scale Ocean-Eddies from Model Data

Author:

NIKOLAUS KOOPMANN

Supervisor:

PROF. DR. CARSTEN

EDEN

2015/03/02

TODO:abstract will be added last...

Contents

Legend	5
1 Introduction	11
1.1 Theory	11
1.2 Important Papers	17
1.3 Methods	20
2 The Algorithm	23
2.1 Step S00: Prepare Data	23
2.2 Step S01b: Find Mean Rossby Radii and Phase Speeds	24
2.3 Step S02: Calculate Geostrophic Parameters	24
2.4 Step S03: Find Contours	25
2.5 Step S04: Filter Eddies	25
2.6 Step S05: Track Eddies	35
2.7 Step S06: Cross Reference Old to New Indices	37
Bibliography	45

Legend

TODO:go through legend

<p>Definition 1: Reynolds Number Re</p> <p>Compares advection of momentum to frictional acceleration.</p> $Re = \frac{UL}{\nu}$	<p>Definition 10: Mechanical Energy per mass $E_k m^2/s^2$</p> <p>Sum of kinetic and potential Energy.</p>
<p>Definition 2: Rossby Number Ro</p> <p>Compares advection of momentum to Coriolis acceleration.</p> $Ro = \frac{U}{fL}$	<p>Definition 11: Rossby Radius $L_R m$</p> <p>The <i>geostrophic wavelength</i>. $L_R = c/f$</p>
<p>Definition 3: Rhines Number R_*</p> <p>Ratio of Rhines scale to horizontal scale.</p> $R_* = \frac{U}{\beta L^2} = \frac{a}{L} Ro$	<p>Definition 12: Steering Level z_S</p> <p>The critical depth where the real part of the Doppler shifted phase speed $c_S(z_S) = c(z) - u(z) = 0$ vanishes. I.e. the depth where the Doppler shift creates a standing wave, causing the disturbances to grow in place instead of spreading in space, analogous to a <i>supersonic bang</i>.</p>
<p>Definition 4: Burger Number Bu</p> <p>Ratio of relative vorticity to <i>stretching</i> vorticity.</p> $\sqrt{Bu} = \frac{NH}{fL} = \frac{L_R}{L}$	
<p>Definition 5: mass $m kg$</p>	
<p>Definition 6: gravitational acceleration $g m/s^2$</p> <p>Value of surface normal component of all body forces.</p>	
<p>Definition 7: vorticity ω_1/s</p>	
<p>Definition 8: Buoyancy Vector B_1/s^2</p> $\mathbf{B} = -\frac{\nabla \rho \times \nabla p}{\rho^2}$	
<p>Definition 9: Kinetic Energy per mass $E_k m^2/s^2$</p>	

Definition 13: Rhines Scale L_r [m]

Scale at which earth's sphericity becomes important.

$$L_r^2 = \frac{U}{\beta} \quad (1)$$

Assuming Gaussian shape:

$$h = A e^{-(x/\sigma)^2/2}$$

$$\text{with } A = a' + a = A e^{-1/2} + a$$

$$\begin{aligned} \frac{\partial h(\sigma)}{\partial x} &= -\frac{A}{\sigma} e^{-1/2} \\ &= -\frac{a'}{\sigma} \end{aligned}$$

hence

$$\begin{aligned} L_r &= \sqrt{\frac{g}{f} \frac{\partial h}{\partial x} \beta} \\ L_r &= \sqrt{\frac{ga'}{f\sigma\beta}} \end{aligned} \quad (2)$$

TODO:en detail:

$$\begin{aligned} \frac{\partial h(\sigma)}{\partial x} &= -\frac{A}{\sigma} e^{-1/2} \\ &= -\frac{a}{\sigma} \frac{e^{-1/2}}{(1 - e^{-1/2})} \\ &= \frac{a}{\sigma (e^{1/2} - 1)} \end{aligned}$$

hence

$$\begin{aligned} L_r &= \sqrt{\frac{g}{f} \frac{\partial h}{\partial x} \beta} \\ L_r &= \sqrt{\frac{g}{e^{1/2} - 1} \frac{a}{f\sigma\beta}} \end{aligned} \quad (3)$$

Definition 14: Gravity Wave Phase Speed cm/s

$$c = \sqrt{g'H}$$

Definition 15: Reduced Gravity

$$g'(x, y, z) \text{m/s}^2$$

$$\text{In the layered model } g' = g \frac{\delta\rho}{\rho_0} = N^2 h$$

Definition 16: Surface/interface Displacement $\eta(x, y)$ m**Definition 17: Brunt Väisälä frequency**

$$N \text{1/s}$$

$$N^2 = g/\rho_0 \frac{\partial \rho}{\partial z}$$

Definition 18: Mean Layer thickness H_m **Definition 19: Layer Thickness/physical height of an isopycnal surface**

$$h(x, y, t) \text{m} / h(x, y, \rho, t) \text{m}$$

$$h = H + \eta \text{ (in the layered model)}$$

Definition 20: Planetary Vorticity $\Omega \text{1/s}$

$$\Omega = 4\pi/\text{day}_{\text{fix}*}$$

Definition 21: Latitude ϕrad **Definition 22: Earth's Radius** a_m **Definition 23: Surface-Normal Planetary Vorticity Component** $f_1 \text{s}$

$$f = f_z = \Omega \sin \phi z$$

Definition 24: Change of Planetary Vorticity with Latitude β_1/ms

$$\beta_1 = \frac{\partial f}{\partial y} = \Omega/a \cos \phi$$

Definition 25: Okubo-Weiss Parameter

$$O_w \text{ 1/s}^2$$

$O_w = \text{divergence}^2 + \text{stretching}^2 + \text{shear}^2 - \text{vorticity}^2$. A negative value indicates vorticity dominated motion, whereas a positive value indicates deformation.
Definition 26: Sea Surface Height SSH m
Definition 27: Isoperimetric Quotient IQ
$IQ = A/A_c = \frac{A}{\pi r_c^2} = \frac{4\pi A}{U^2} \leq 1$. The ratio of a ring's area to the area of a circle with equal circumference.
Definition 28: Gaussian radius σ m
$(H - a) = H \exp\left(-\frac{A}{2\pi\sigma^2}\right)$. Twice the Gaussian standard-deviation. a: amplitude H: Gaussian amplitude A: determined area
Definition 29: dynamic eddy scale σ m
Distance from eddy's center to the line of maximum orbital speed <i>i.e.</i> the zero-vorticity contour.

Definition 30: Run $aviso\text{-}MI$ 7-day time-step $aviso$ with method MI.
Definition 31: Run $aviso\text{-}MII$ 7-day time-step $aviso$ with method MII.
Definition 32: Run $pop2avi\text{-}MII$ 7-day time-step POP remapped to $aviso$ -geometry with method MII.
Definition 33: Run $POP\text{-}7day\text{-}MII$ 7-day time-step POP with method MII.
Definition 34: Run $POP\text{-}1day\text{-}MII\text{-}Southern\text{-}Ocean$ 1-day time-step $aviso$ with method MII. Southern Ocean Only. Minimum Age: 30 d Contour step raised to 2 cm
Definition 35: Parallel Ocean Program (POP). Global fully non-linear $0^{\circ}6'$, 1 d, primitive equation ocean model Oestreicher (n.d.) .
Definition 36: TODO:AVISO Forget (2010)

1

Introduction

THE MAIN PURPOSE of this study is to create a computer program that is able to **detect**, **track** and **analyse** meso-scale ocean eddies via their surface signal in sea-surface-height (SSH). Due to the inherently technical character of the matter, large parts are dedicated to technicalities of the algorithm ¹. Oceanographic results are treated in the [results](#)- and [discussion](#)-chapters. This chapter discusses the physics of meso-scale geostrophic turbulence and introduces a handful of relevant historical papers. Since focus is on horizontal scales, translational speeds and the comparison of results between the [AVISO](#)-altimetry product and SSH-data from the [POP](#) ocean model, sections generally focus on either of these three topics.

1.1 Theory

THIS section discusses the theory of meso-scale turbulence and parametrizations thereof. Geostrophic turbulence is typically characterized by rather stable, circular, coherent pressure anomalies, that rotate fluid around in a vortex in quasi-geostrophic equilibrium. These entities can persist for long periods of time in which they often travel distances on the order of hundreds of kilometers zonally. The fact that baroclinic instability leads to these vortices, instead of cascading to ever smaller scales as would be expected from chaotic turbulence, is a direct consequence of the inverse energy cascade of two-dimensional motion² (see ??.). The atmospheric analog are

¹ see the methods-chapter 2.

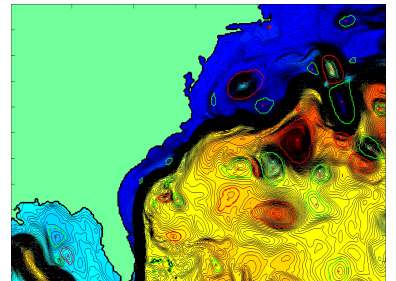


Figure 1.1: Animation snapshot of early test run. Shown is SSH with detected eddies indicated by red and green lines.

² For a discussion of this phenomenon see ??

storms and high-pressure systems, yet with much less difference between high- and low-pressure systems due to a smaller centrifugal force *i.e.* smaller Rossby number (Ro). These quasi-geostrophic, meso-scale vortices, from here on called eddies³, are immediately visible on SSH-maps (see **TODO:fig of map-minus mean(SSH)**). Yet, it is difficult to physically *define* an eddy in terms of oceanographic variables. The transition from meandering jets or other undeveloped baroclinic turbulence to a coherent vortex is not very sharp. Eddies also sometimes merge or split or collectively form rifts and valleys in SSH. Detecting them on one snapshot automatically via an algorithm is therefore not trivial. Further problems arise when the algorithm is also supposed to track each individual over time. Their sheer abundance at any given time inevitably creates ambiguities as to *which is which* between time steps.

TODO:do O_w over!

1.1.1 Detection methods

- One way to find an eddy in SSH-data is to simply scan for closed contours at different values for z and then subject found entities to a series of geometric tests. Only if all criteria are met is an eddy found. This method was first used by [Chelton et al. \(2011\)](#) and is certainly a relatively simple yet very effective method, at least so for satellite data. Therefore, as a starting point, this method will be adopted and should also serve as a general definition of what will be referred to as an *eddy* hereafter⁴.

[Chelton et al.](#) set the following threshold criteria for his algorithm:

1. The SSH values of all of the pixels are above (below) a given SSH threshold for anticyclonic (cyclonic) eddies.
2. There are at least $[threshold]$ pixels and fewer than $[threshold]$ pixels comprising the connected region.
3. There is at least one local maximum (minimum) of SSH for anticyclonic (cyclonic) eddies.
4. The amplitude of the eddy is at least $[threshold]$.
5. The distance between any pair of points within the connected region must be less than $[threshold]$.

³ For a discussion of the different types of vortices in the ocean see appendix ??

⁴ The vortices will have names deviant from *eddy* where these criteria are altered.

- Another frequently used method to define an eddy makes use of the strain tensor ⁵ \mathbf{T} . The trace of the strain tensor squared includes valuable information about the dynamics of the velocity field. Namely

$$2\mathbf{O}_W = \text{Tr } \mathbf{T}^2 = \text{divergence}^2 + \text{stretching}^2 + \text{shear}^2 - \text{vorticity}^2 \quad (1.1)$$

⁵ see [Derivation ??](#)

which reduces to $\mathbf{O}_W = (\partial_x u)^2 + 2\partial_y u \partial_x v$ in two dimensions. This is called the Okubo-Weiss-Parameter ([Okubo, 1970](#)). It is a useful tool to determine whether the field has parabolic, vorticity dominated character, or whether deformation dominates, giving hyperbolic character. An area of large negative values indicates high enstrophy density compared to gradients of kinetic energy, thus indicating little friction paired with high momentum *i.e.* a coherent, angular-momentum-conserving entity. Positive values on the other hand indicate incoherent deformation.

As ingenious as this parameter seems, it turns out that using it to identify eddies is often not the best solution. [Chelton et al. \(2011\)](#) name 3 major drawbacks:

- *No single threshold value for \mathbf{O}_W is optimal for the entire World Ocean. Setting the threshold too high can result in failure to identify small eddies, while a threshold that is too low can lead to a definition of eddies with unrealistically large areas that may encompass multiple vortices, sometimes with opposite polarities.*
- *\mathbf{O}_W is highly susceptible to noise in the SSH field. Especially when velocities are calculated from geostrophy, the sea surface has effectively been differentiated twice and then squared, exacerbating small incontinuities in the data.*
- *The third problem with the W-based method is that the interiors of eddies defined by closed contours of W do not generally coincide with closed contours of SSH. The misregistration of the two fields is often quite substantial.*

It is hence only logical to scan for closed contours of SSH directly (as was done so by [Chelton et al.](#)).

1.1.2 *Eddy Drift Speeds*

Intuitively any translative motion of a vortex should stem from an asymmetry of forces as in an imperfectly balanced gyroscope wobbling around and translating across a table. The main effects that cause a quasi-geostrophic ocean eddy to translate laterally can rel. easily be explained heuristically.

Box 1. Lateral Density Gradient

Consider a mean layer-thickness gradient $\frac{\partial h}{\partial x} > 0$ somewhere in the high northern latitudes and a geostrophic, positive density anomaly within that layer. In other words, a high-pressure vortex or an anti-cyclonic eddy with length scale $L \approx L_R$. Hence a vorticity budget dominated by advection of relative vorticity and vortex stretching.

Next consider a parcel of water within the eddy's western flank. As the clockwise rotating eddy advects the parcel east via its northern side the water-column comprising said fluid will be stretched vertically as it is advected towards larger depths. In order to maintain total vorticity a small new relative-vorticity term is introduced. Since the vorticity budget is dominated by the planetary component, this new term has sign of f , i.e. positive. The net effect is that the absolute value of the parcel's (negative) relative vorticity is reduced i.e. the circular flow around the eddy's center is slowed (via term C in equation (??)), leading to an accumulation of water on the eddy's northern flank.

The opposite effect holds for a parcel advected along the southern side from east to west. Then, total (positive) vorticity is reduced so that the already negative relative vorticity becomes even more *negative*, resulting in an accelerated flow south to the eddy's core. To conserve volume the accumulation north and the decumulation of water south, the eddy is slowly pushed south.

Note that the rotational sense of the eddy is irrelevant here. In the cyclonic case, even though columns are stretched north and south directly opposite to the anti-cyclonic case, the effect on absolute values of relative vorticity is directly opposite too. I.e. vortex stretching, even though now in the south, now increases the flow, as the added term of rel. vorticity now is of the same sign as the eddy itself.

The drift direction is hence dictated by the sign of f , so that eddies in the northern hemisphere will be pushed along gradients with the shallower water always on their right and vice versa on the southern hemisphere.

Box 2. Planetary Lift

Assume now that βL be comparable or larger even than $f_0 - \omega$ from the previous example. Then, all fluid adjacent to the eddy on its northern and southern flanks will be transported meridionally, thereby be tilted with respect to Ω and hence acquire relative vorticity to compensate. All fluid transported north will balance the increase in planetary vorticity with a decrease in relative vorticity and vice versa for fluid transported south. This is again independent of the eddy's sense and in this case also independent of hemisphere since $\frac{\partial f}{\partial y} = \beta > 0$ for all latitudes. The result is that small negative vortices to the northern and small positive vortices to the southern flank of eddies will push them west.

Box 3. Eddy-Internal β -Effect

In the later case clearly particles within the vortex undergo a change in planetary vorticity as well. Or from a different point of view, since $U \sim \nabla p/f$, and noting that the pressure gradient is the driving force here and hence fix at first approximation, particles drifting north will decelerate and those drifting south will accelerate. In order to maintain mass continuity, the center of volume will be shifted west for an anti-cyclone and east for a cyclone. Another way to look at it is to note that the only way for the discrepancy in Coriolis acceleration north and south, whilst maintaining constant eddy-relative particle speed, is to superimpose a zonal drift velocity so that net particle velocities achieve symmetric Coriolis acceleration.

TODO:equations to follow Cushman-Roisin (1990) van Leeuwen (2007)

1.1.3 The Integral Length Scale of Turbulence

1.1.3.0.1 This section is intended to shed light on the benefits of exact determinations of ocean-eddy-scales. That is, their horizontal extent *i.e.* their diameter or *wavelength*.

1.1.3.0.2 Just like the *eddy* itself, its scale is rather vague and difficult to define. What physical parameter defines the outer edge of a seamless, smooth vortex? If the eddy is detected as done by Chelton *et al.* (2011), *i.e.* closed contours of SSH the interior of which fulfilling certain criteria, the measured perimeter may jump considerably from one time step to the next. An incremental difference in the choice of z might translate to a perimeter outlining twice the difference in area, especially when SSH gradients are small.

Another possibility is to define an amplitude first, then assume a certain shape *e.g.* Gaussian, and then infer the radius indirectly. The obvious problem with this approach would be to properly define the amplitude.

The most physically sound method would have to be one depending on the eddy's most defining physical variable, that is unambiguously determinable from SSH. The geostrophic velocities. Chelton *et al.* (2011), as with everything else, tried all methods but also conclude that the later is the most adequate one. ⁶**TODO:ref to technical chapter.**

1.1.3.0.3 Construed as an integral length scale of turbulence *i.e.* as the distance at which the auto-correlation of particles reaches zero, the *eddy-scale* turns out to be of fundamental relevance for attempts to parametrize geostrophic turbulence.

General circulation models ($\mathcal{O}(10^2)$ km) as they are used in *e.g.* climate forecasts are too coarse to resolve meso-scale ($\mathcal{O}(10^1)$ km) turbulence. Even if the Von-Neumann-condition were ignored and a refinement were desired horizontally only, a leap of one order of magnitude would cause an increase in calculation time of factor ⁷ $x = 100$. The effects of the non-linear terms therefore have to be somehow articulated in an integral sense for the large grid-boxes in the model. A common approach is to assume that *eddy kinetic energy* $\overline{u'u'}$ and *eddy potential energy* $\overline{w'p'}$, akin to diffusive processes ⁸, are

⁶ See Chapter

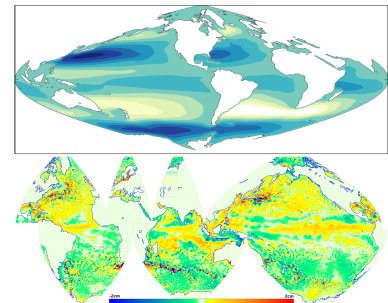


Figure 1.2: top: Stommel's equation $\mathcal{F}_{\text{bottom}} - \mathcal{F}_{\text{surface}} = -v\beta$ with constant eddy viscosity. bottom: Parallel Ocean Program eddy-resolving model snapshot with SSH mean of one year subtracted.

⁷ With the Moore's-Law-type exponential growth in FLOP/S of the last 22 years for supercomputers ($\lg(x) \sim 3/11a$) a factor 100 interestingly translates to only $a = 22/3 \approx 7$ years...

⁸ In analogy to Fick's first law of diffusion

proportional to the gradient of \bar{u} respective \bar{b} (down-gradient-parametrization⁹) (Olbers *et al.*, 2012), which leads to the problem of finding expressions for the *turbulent diffusivities i.e.* the rate at which gradients are diffused by turbulence. This parameter is by no means constant, instead it can span several orders of magnitude, itself depending on the strength of turbulence-relevant gradients, and sometimes even assuming negative values (Eden & Greatbatch, 2008). Precise knowledge of the integral length scale and the physics that set it is hence vital for attempts to analyze and set values for eddy diffusivities and turbulence parametrizations in general.

⁹ *i.e.* Reynolds averaging

1.2 Important Papers

1.2.1¹⁰

Rhines investigated the effect of the β -plane on the inverse energy cascade of quasi-2-dimensional atmospheric and oceanic turbulence. At constant f , energy should be cascaded to ever-larger scales until halted by the scale of the domain. This is clearly not the case, as no storm has ever grown to global scale. The presence of a meridional restoring force creates a critical scale beyond which the *turbulent migration of the dominant scale nearly ceases* . . . Instead, Rossby waves are excited which would theoretically eventually give way to alternating zonal jets of width L . This scale was later coined the Rhines Scale.

¹⁰ Rhines, Peter B. 1974. Waves and turbulence on a beta-plane. *J. Fluid Mech.*, **69**(03), 417

1.2.2¹¹

Bjerknes & Holmboe (1944) already noted that the β -effect causes a mass-imbalance in planetary vortices that, if not met by an asymmetry in shape must lead to westward propagation. Nof (1981) derived that the β -effect results in a net meridional force on the integrated mass of the vortex, which in balance with the Coriolis acceleration shoves cyclones eastward and anti-cyclones westward. They also explained how displaced water outside the eddy's perimeter causes a much stronger westward component, with the result that all eddies propagate westward irrespective of rotational sense. The westward

¹¹ Cushman-Roisin, B. 1990. Westward motion of mesoscale eddies. *J. Phys.* . . .

drift was also derived in various forms by *e.g.* [Flierl \(1984\)](#); [Matsuura & Yamagata \(1982\)](#).

[Cushman-Roisin \(1990\)](#) put it all into a less restricted uniform formalism by scaling the terms in the one-layer primitive equations by their respective dimensionless numbers. By integrating the interface-displacement caused by the eddy over the eddy's domain and applying mass continuity they derived for the location (X, Y) of an eddy's centroid¹²:

$$\begin{aligned}\Pi X_{tt} - Y_t &= L_R T \beta \langle yv \rangle + L \frac{\beta}{f} \langle y\eta v \rangle \\ \Pi Y_{tt} - X_t &= -L_R T \beta \langle yu \rangle - L \frac{\beta}{f} \langle y\eta u \rangle\end{aligned}\quad (1.2)$$

¹² $\langle \rangle \equiv \frac{1}{A} \int_A dA$

where $\Pi = 1/f_0 T$.

Hence, independent of balance of forces the eddy's center of mass describes inertial oscillations¹³ on the f -plane, even in the absence of β . Using geostrophic values for u and returning to dimensional variables equation (1.2) can be cast into:

$$X_t = \frac{\omega_{\text{long}}}{k} \left(1 + \frac{1}{H} \frac{\int \eta^2 dA}{2V_e} \right) \quad (1.3)$$

The first term represents the ?? from [1.1.2](#), whereas the second term represents the ?? . Note that the first term is always westwards, while the second has sign of $-\eta$, *i.e.* westward for anti-cyclones and eastward for cyclones and that the first is always larger than the second. **TODO:van Leeuwen (2007) for derivation if time**

¹³ compare to *harmonic oscillator*

1.2.3 Early Altimeter Data

The advent of satellite altimetry, which Walter Munk called *the most successful ocean experiment of all time* [Orbach & Munk \(2002\)](#), finally allowed for global-scale experimental investigations of oceanic planetary phenomena on long time- and spatial scales. Among others, [Matano et al. \(1993\)](#); [Cipollini et al. \(1997\)](#); [Le Traon & Minster \(1993\)](#) were the first to use satellite-data to present evidence for the existence of Rossby waves and their westward-migration in accord with theory. Surprisingly all of the observations found the phase speeds to be 1 to 1.5 times larger than what theory predicted. Several theories to explain the discrepancy were presented. *E.g.* [Killworth et al.](#)

(1997) argued that the discrepancy was caused by mode-2-east-west-mean-flow velocities. Interestingly it appears that hitherto, the relevant altimeter signal was mainly associated with linear waves. Non-linearities are rarely mentioned in the papers of those years. Probably simply due to the fact that the turbulent character of much of the meso-scale variability was still obscured by the poor resolution of the first altimeter products.

1.2.4 SSH Altimeter Data ¹⁴

From the beginning of satellite altimetry Chelton *et al.* have invested tremendous effort to thoroughly analyze the data in terms of Rossby waves and geostrophic turbulence. At the time of the Killworth *et al.* (1997) paper only 3 years of Topex/Poseidon data alone had been available, which led them to interpret the data mainly in terms of Rossby waves. Once the merged Aviso T/P and ERS 1/2 **TODO:ref** was released 7 years later, Chelton *et al.* presented a new analysis that was based on an automated eddy-tracking algorithm using the geostrophic Okubo-Weiss parameter ^{15,16}. For the first time Satellite data was sufficiently fine resolved to unveil the dominance of *blobby* (*sic*) structures rather than latitudinally β -refracted continuous crests and troughs that had hitherto been assumed to characterize the large scale SSH picture. They presented results of a refined algorithm in their 2011 paper, in which they abandoned the Okubo-Weiss concept and instead identified eddies via closed contours of SSH itself ¹⁷. Among their most significant findings is the conclusion that on the one hand, the vast majority of extra-tropical west-ward propagating SSH-variability consists of coherent, isolated, non-linear, meso-scale eddies, whilst on the other hand, these eddies propagate about 25% slower ¹⁸ than small amplitude features of larger lateral scale, that are difficult to separate from the data and are assumed to obey linear Rossby wave theory. **TODO:rephrase** Apart from this they find little evidence for any dispersion in the signal, neither do they find evidence for significant meridional propagation, as should be found for Rossby waves. In agreement with Rhines & Holland (1979), they find this eddy-dominated regime to fade in vicinity of the equator, giving way to the characteristic Rossby-wave profile. Almost all of their eddies propagate

¹⁴ Chelton, Dudley B., Schlax, Michael G., Samelson, Roger M., & de Szoeke, Roland a. 2007. Global observations of large oceanic eddies. *Geophys. Res. Lett.*, **34**(15), L15606; and Chelton, Dudley B., Schlax, Michael G., & Samelson, Roger M. 2011. Global observations of nonlinear mesoscale eddies. *Prog. Oceanogr.*, **91**(2), 167–216

¹⁵ see section 1.1.1

¹⁶ see Derivation ??

¹⁷ note that geostrophic O_W is a second derivative of SSH and thus exacerbates noise in the SSH data.

¹⁸ pointing to dispersion.

westwards. Those that are advected eastwards by *e.g.* the ACC show significantly shorter life-times than those that are not. For more detail on their results and a discussion of the limitations of eddy-tracking via satellites see section ??.

1.3 Methods

1.3.1 Satellite vs Model Data

1.3.1.0.4 Satellites The latest Aviso SSH data from satellites features impressive accuracy, constancy and resolutions in both space and time. This is achieved by collecting all of the data from all of the altimeter-equipped satellites available at any given moment for any given coordinate. This conglomerate of highly inhomogeneous data is then subjected to state-of-the-art interpolation methods to produce a spatially and temporally coherent product. One satellite alone is not sufficient to adequately resolve meso-scale variability globally. Take *e.g.* the Topex/Poseidon satellite.

It had a ground repeat track orbit of 10 days and circled the earth in 112 minutes or ≈ 13 times a day with a swath width of 5 km. Hence it drew ≈ 26 5 km-wide stripes onto the globe every day. This pattern is then repeated after 10 days, which means that at the equator only $10 \times 26 \times 5 = 1300$ km of the $2\pi \times 6371 = 40000$ km get covered, *i.e.* 3.25%. At every 10d time step, on average, effectively $40000/1300 - 5 = 20$ km are left blank in-between swaths on the equator. This is why, no matter how fine the resolution within the swath at one moment in time may be, the spatial resolution is so coarse.

The merged ERS-1/Topex-data as used by [Chelton et al. \(2011\)](#) has a time step of 7 days. Assuming eddy drift speeds of $u_e = 0$ (10^{-1}) m/s implies a distance traveled per time step of $L_{\delta t} \approx 60$ km. [Chelton et al.](#) estimate their effective spatial resolution as $\delta x \approx 40$ km. Eddies of smaller scale are not resolved. Tracking a single eddy from one time-step to the next should hence be feasible, especially when u_e is approximately known. Problems arise when the sea level is characterized by an abundance of isolated vortices plus maybe even further meso-scale noise of comparable amplitude.

Ambiguities arise in terms of correctly matching the eddies

	POP	merged T/P - ERS-1
dx	7km – 11km	$1/3^\circ$ (≈ 40 km after filtering)
dt	1d	7d
$\log_{10} 2$ filter cutoff	n/a	2° by 2°
z-levels	42	1
variables	SSH,S,T,u,v	SSHFacers
pot. interpolation artifacts	n/a	yes
reality	no	yes

Table 1.1: [5pt]model vs satellite data

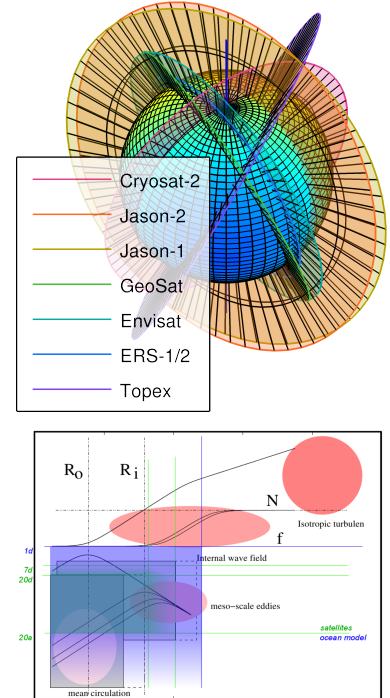


Figure 1.3: Resolutions for model vs satellite. Modified version from [Olbers et al. \(2012\)](#).

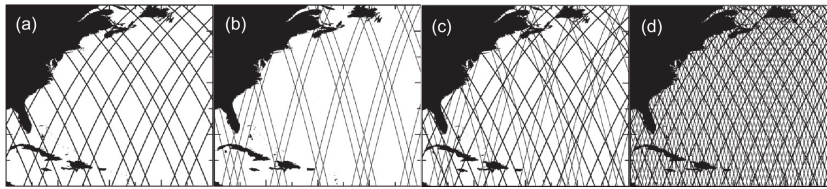
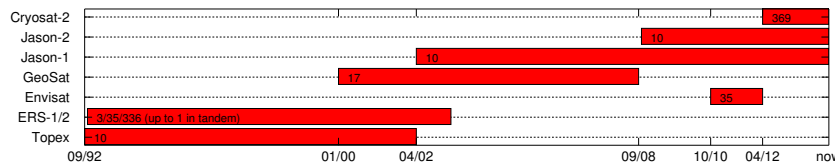


Figure 1.4: The ground track patterns for the 10-day repeat orbit of T/P and its successors Jason-1 and Jason-2 (thick lines) and the 35-day repeat orbit of ERS-1 and its successors ERS-2 and Envisat (thin lines). (a) The ground tracks of the 10-day orbit during a representative 7-day period; (b) The ground tracks of the 35-day orbit during the same representative 7-day period; (c) The combined ground tracks of the 10-day orbit and the 35-day orbit during the $^{19}(\delta)^{10^1} \text{ km/day}$ 7-day period, and (d) The combined ground tracks of the 10-day orbit and the 35-day orbit during the full 35 days of the 35-day orbit. (sic) Chelton *et al.* (2011)

from the old time-step with those in the new one, potentially causing aliasing effects in the final statistics. The translational speeds ¹⁹ of eddies are not really the problem here, as they usually drift slow enough to not cover more than 1 grid node per 7 day time step. The issue are those areas where eddies are born, die and merge. According to Smith & Marshall (2009) instabilities within the ACC grow at rates of up to $1/(2\text{days})$, which means that at a time-step up to 3 eddies have emerged and equally many died for every eddy identified within such region. The ground-repeat frequency of a satellite can of course not be set arbitrarily. Especially when the satellite is desired to cover as far north and south as possible, whilst still being subjected to just the right torque from the earth's variable gravitational field to precess at preferably a sun-synchronous frequency *i.e.* $360^\circ/\text{year}$. Neither can the satellite's altitude be chosen arbitrarily. If too low the oblateness of the earth creates too much eccentricity in the orbit that can no longer be *frozen* ²⁰. Another problem could be potential inhomogeneity in the merged data in time dimension, since products of old and current missions are lumped together into one product. This is why Chelton *et al.* (2011) opted against the finest resolution available and instead went for a product that had the most satellites merged in unison for the longest period of time.



²⁰ minimizing undulating signals in altitude by choosing the right initial values.

Figure 1.5: Length of mission. Numbers are orbit-period in days.

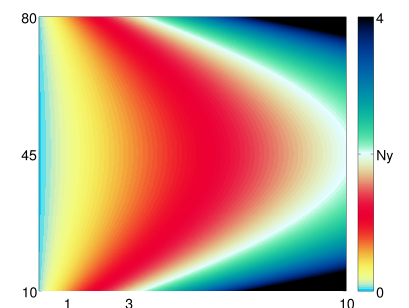


Figure 1.6: $\epsilon(\phi, \mu)$. $Ny \equiv 2$ *i.e.* the Nyquist frequency.

1.3.1.0.5 Ocean Model The advantages of detecting and tracking eddies from model data are obvious. Say you have $Bu = 1$, so that $L = NH/f$. Let's assume ²¹ $NH = a/10d$, a model resolution of $1^\circ/\mu$ and that the eddy diameter was twice the Rossby radius. How many grid notes ξ fit into one eddy as a function of latitude?

$$\xi = \frac{a \cos \phi}{2\pi} = \frac{2NH}{f} = \frac{2NH1d}{4\pi \sin(\phi)}$$

$$\xi = \frac{2\mu}{10 \sin(2\phi)} \quad (1.4)$$

See figure 1.6 for the results. In this flat-bottom, constant ρ_z , Mercator-gridded model the worst eddy-resolution is interestingly at mid-latitude. A value of $\xi > 2$ is desirable, because it eradicates ambiguities in the tracking procedure, with the result that there is no need to *forecast* the position x_e of an eddy for the new time step. It suffices to determine the closest eddy from the previous time-step for respective eddy from the new time step and vice versa. Those 2 eddies that are in agreement are successfully matched, those from the new (old) time step that do not find a match have just been born (have died). See also section **TODO:ref to section** for the technical stuff. Another major advantage of the model is that it produces not only SSH data but also all other relevant variables ²², for not only the surface but for many different depths. The surface velocities inferred from altimetry are the geostrophic components only, which should suffice to *e.g.* determine the non-linearity and kinetic energy of an eddy for almost all regions, but less so for *e.g.* the western boundary currents. The *one* draw-back of using model data is that, in contrast to the satellite data, it does not represent reality. **TODO:to be continued**

²¹ corresponds to $L(\phi = 30^\circ) = 100\text{km}$

²² See section ?? for all the possibilities that arise.

2

The Algorithm

This section walks through the algorithm step by step, so as to explain which methods are used and how they are implemented. The idea is that the code from step `S00..` on can only accept one well defined structure of data. In earlier versions the approach was to write code that would adapt to different types of data automatically. All of this extra adaptivity turned out to visually and structurally clog the code more than it did offer much of a benefit. The concept was therefore reversed. `S00_prep_data` can be altered to produce required output. Yet, there should be no need to adapt any of the later steps in any way. All input parameters are to be set in `INPUT.m` and `INPUTxxx.m`.

2.1 Step S00: Prepare Data

```
function S00_prep_data
```

Before the actual eddy detection and tracking is performed, SSH-, latitude- and longitude-data is extracted from the given data at desired geo-coordinate bounds and saved as structures in the form needed by the next step (S01). This step also builds the file `window.mat` via `GetWindow3` which saves geometric information about the input and output data as well as a cross-referencing index-matrix which is used to reshape all *cuts* to the user defined geo-coordinate-geometry. The code can handle geo-coordinate input that crosses the longitudinal seam of the input data. E.g. say the input data comes in matrices that start and end on some (not necessarily strictly meridional) line straight across the Pacific and it is the Pacific only that

is to be analyzed for eddies, the output maps are stitched accordingly. In the zonally continuous case *i.e.* the full-longitude case, an *overlap* in x-direction across the *seam*-meridian of the chosen map is included so that contours across the seam can be detected and tracked across it. One effect is that eddies in proximity to the seam can get detected twice at both zonal ends of the maps. The redundant *ghost*-eddies get filtered out in `S05_track_eddies`.

2.2 Step S01b: Find Mean Rossby Radii and Phase Speeds

```
function S01b_BruntVaisRossby
```

This function...

- – ...calculates the pressure $P(z, \phi)$ in order to...
 - ...calculate the Brunt-Väisälä-Frequency according to $N^2(S, T, P, \phi) = -\frac{g(\phi)}{P} \frac{\partial \rho(S, T, P)}{\partial z}$ in order to...
- – ...integrate the Rossby-Radius $L_R = \frac{1}{\pi f} \int_H N dz$ and ...
 - apply the long-Rossby-Wave dispersion relation to found L_R to estimate Rossby-Wave phase-speeds $c = -\frac{\beta}{k^2 + (1/L_R)^2} \approx -\beta L_R^2$

The 3-dimensional matrices (S and T) are cut zonally into slices which then get distributed to the threads. This allows for matrix operations for all calculations which would otherwise cause memory problems due to the immense sizes of the 3d-data ¹.

¹ E.g. the pop data has dimensions $42 \times 3600 \times 1800$.

2.3 Step S02: Calculate Geostrophic Parameters

```
function S02_infer_fields
```

This step reads the cut SSH data from `S00_prep_data` to perform 2 steps:

1. Calculate a mean over time of $\text{SSH}(y, x)$.
2. • use one of the files' geo-information to determine f, \dots, g and the ratio g/f .
 - calculate geostrophic fields from SSH gradients.
 - calculate deformation fields (vorticity, divergence, stretch and shear) via the fields supplied by the last step.

- calculate O_w .
- Subtract the mean from step 1 from each $SSH(t)$ to filter out persistent SSH -gradients *e.g.* across the Gulf-Stream.

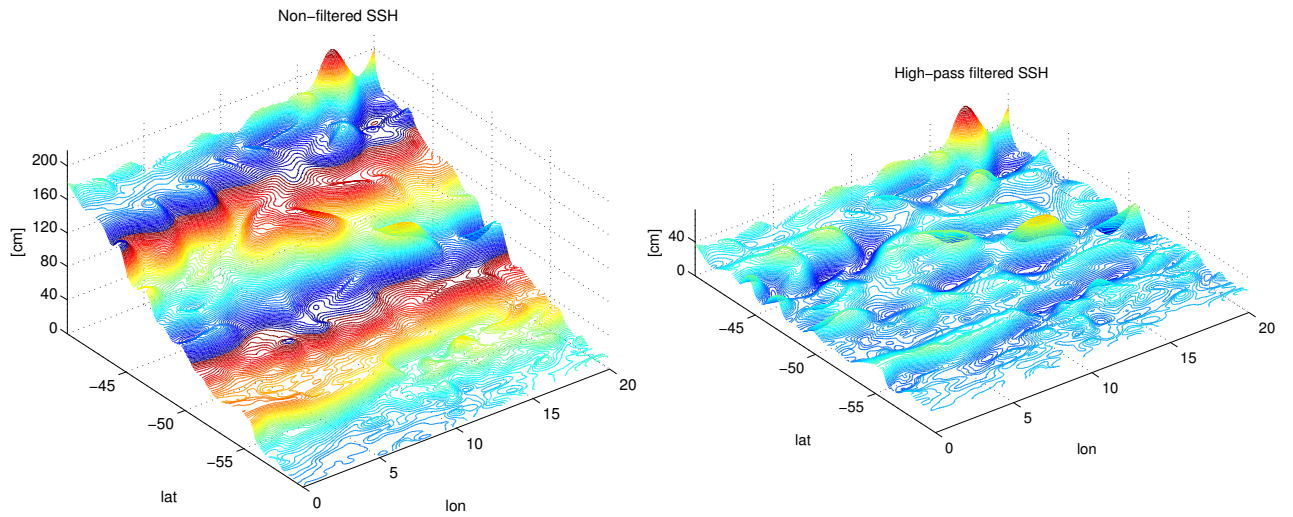


Figure 2.1: SSH with mean over time subtracted.

2.4 Step S03: Find Contours

```
function S03_contours
```

The sole purpose of this step is to apply MATLAB's `contourc.m` function to the SSH data. It simply saves one file per time-step with all contour indices appended into one vector². The contour intervals are determined by the user defined increment and range from the minimum- to the maximum of given SSH data.

The function `initialise.m`, which is called at the very beginning of every step, here has the purpose of rechecking the *cuts* for consistency and correcting the time-steps accordingly (*i.e.* when files are missing). `initialise.m` also distributes the files to the threads *i.e.* parallelization is in time dimension.

² see the MATLAB documentation.

2.5 Step S04: Filter Eddies

```
function S04_filter_eddies
```

Since indices of all possible contour lines at chosen levels are available at this point, it is now time to subject each and every contour to a myriad of tests to decide whether it qualifies as the outline of an eddy as defined by the user input threshold parameters.

2.5.1 Reshape for Filtering and Correct out of Bounds Values

```
function eddies2struct
function CleanEddies
```

In the first step the potential eddies are transformed to a more sensible format, that is, a structure `Eddies(EddyCount)` where `EddyCount` is the number of all contours. The struct has fields for level, number of vertices, exact *i.e.* interpolated coordinates and rounded integer coordinates.

The interpolation of `contourc.m` sometimes creates indices that are either smaller than 0.5 or larger than $N + 0.5$ ³ for contours that lie along a boundary. After rounding, this seldomly leads to indices of either 0 or $N + 1$. These values get set to 1 and N respectively in this step.

³where N is the domain size

2.5.2 Descent/Ascend Water Column and Apply Checks

```
function walkThroughContsVertically
```

The concept of this step is a direct adaption of the algorithm described by [Chelton *et al.* \(2011\)](#). It is split into two steps, one for anti-cyclones and one for cyclones. Consider *e.g.* the anti-cyclone situation. Since all geostrophic anti-cyclones are regions of relative high pressure, all anti-cyclones⁴ effect an elevated `SSH` *i.e.* a *hill*. The algorithm ascends the full range of `SSH` levels where contours were found. Consider an approximately Gaussian shaped AC that has a peak `SSH` of say 5 increments larger than the average surrounding waters. As the algorithm approaches the sea surface from below, it will eventually run into contours that are closed onto themselves and that encompass the AC. At first these contours might be very large and encompass not only one but several ACs and likely also cyclones, but as the algorithm continues upwards found contour will get increasingly circular, describing some outer *edge* of the AC. Once the contour and its interior pass all of the tests the algorithm will decide that an AC was found and

⁴abbreviated AC henceforth

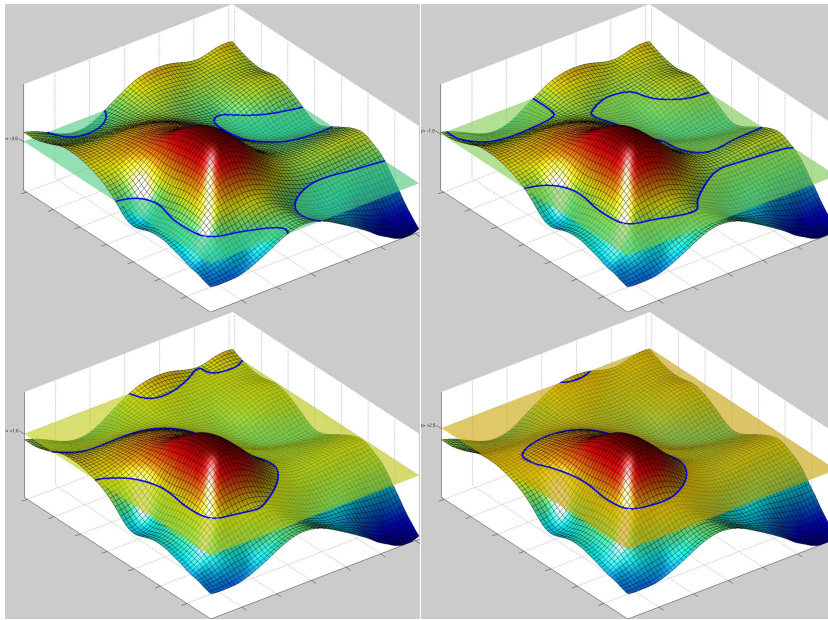


Figure 2.2: TODO:YO!

write it and all its parameters to disk. The AC's region *i.e.* the interior of the contour will be flagged from here on. Hence any inner contour further up the water column will not pass the tests. Once all AC's are found for a given time-step, the SSH flags get reset and the entire procedure is repeated only this time *descending* the SSH-range to find cyclones. The tests for cyclones and anti-cyclones are identical except for a factor -1 where applicable. In the following the most important steps of the analysis are outlined.

Contour filter 1 NaN-Check Contour

```
function CR_RimNan
```

The first and most efficient test is to check whether indices of the contour are already flagged. Contours within an already found eddy get thereby rejected immediately.

Contour filter 2 Closed Ring

```
function CR_ClosedRing
```

Contours that do not close onto themselves are obviously not eligible for further testing.

Contour filter 3 Sub-Window

```
function get_window_limits, EddyCut_init
```

For further analysis a sub-domain around the eddy is cut out of the SSH data. These functions determine the indices of that window and subtract the resultant offset for the contour indices.

Contour filter 4 Logical Mask of Eddy Interiour

```
function EddyCut_mask
```

Basically this function creates a **flood-fill** logical mask of the eddy-interior. This is by far the most calculation intensive part of the whole filtering procedure. A lot more time was wasted on attempting to solve this problem more efficiently than time could have been saved would said attempts have been successful. The current solution is basically just MATLAB's `imfill.m`, which was also used in the very first version of 09/2013. EDIT: `imfill.m` was replaced by using `inpoly.m` to determine which indices lie within the contour-polygon. This method seems to be more exact at determining whether the inside-part of one grid cell (with respect to the smooth, spline-interpolated contour) is larger than the outside part or not.

Contour filter 5 Sense

```
function CR_sense
```

All of the interior SSH values must lie either above or below current contour level, depending on whether anti-cyclones or cyclones are sought.

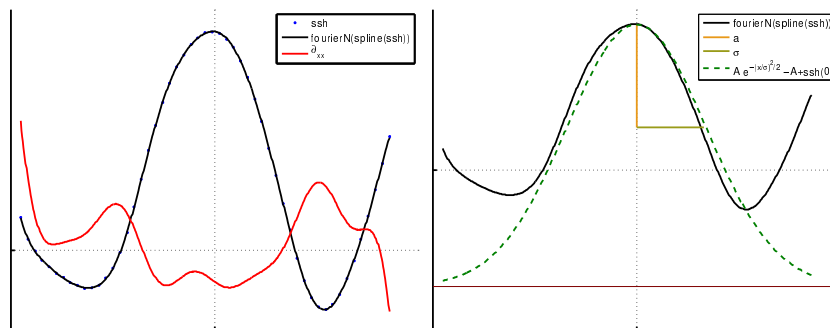


Figure 2.3: Left: Fourier-fit of an eddy from POP-SSH-data and the 2nd differential thereof. Right: Theoretical Gauss-Shape built from the resulting *standard-deviation* i.e. σ and amplitude.

Contour filter 6 Area

```
function getArea
```

The main goal here is to determine the area encompassed by the exact coordinates of the contour. It does so via MATLAB's `polyarea` function. This area is not related to the scale σ that is determined in 12. It is however the relevant scale for the determination of the isoperimetric quotient in 8.

If the respective switch is turned on, this function also checks that the area of found contour does not surpass a given threshold which in turn is a function of L_R . Since L_R gets very small in high latitudes a lower bound on the L_R used here should be set as well. This is especially important for the southern ocean where L_R gets very small while the strong meso-scale turbulence of the Antarctic circumpolar current results in an abundance of relatively large eddies as far south as 60°S and beyond.

Contour filter 7 Circumference

```
function EddyCircumference
```

Circumference *e.g.* line-length described by the contour. This is the other parameter needed for 8. This is however neither related to the actual eddy scale determined in 12.

Contour filter 8 Shape

```
function CR_Shape
```

This is the crucial part of deciding whether the object is *round enough*. A perfect vortex with $\frac{\partial u}{\partial y} = -\frac{\partial v}{\partial x}$ is necessarily a circle. The problem is that eddies get formed, die, merge, run into obstacles, get asymmetrically advected etc. To successfully track them it is therefore necessary to allow less circle-like shapes whilst still avoiding to *e.g.* count 2 semi merged eddies as one. This is achieved by calculating the **isoperimetric quotient**, defined as the ratio of a ring's area to the area of a circle with equal circumference. [Chelton et al. \(2011\)](#) use a similar method. They require:

The distance between any pair of points within the connected region must be less than a specified maximum [Chelton et al. \(2011\)](#).

While this method clearly avoids overly elongated shapes it allows for stronger deformation within its distance bounds.

Contour filter 9 Amplitude

```
function CR_AmpPeak
```

This function determines the amplitude *i.e.* the maximum of

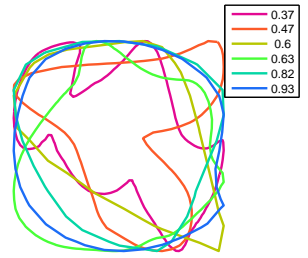


Figure 2.4: Different values of the isoperimetric quotient.

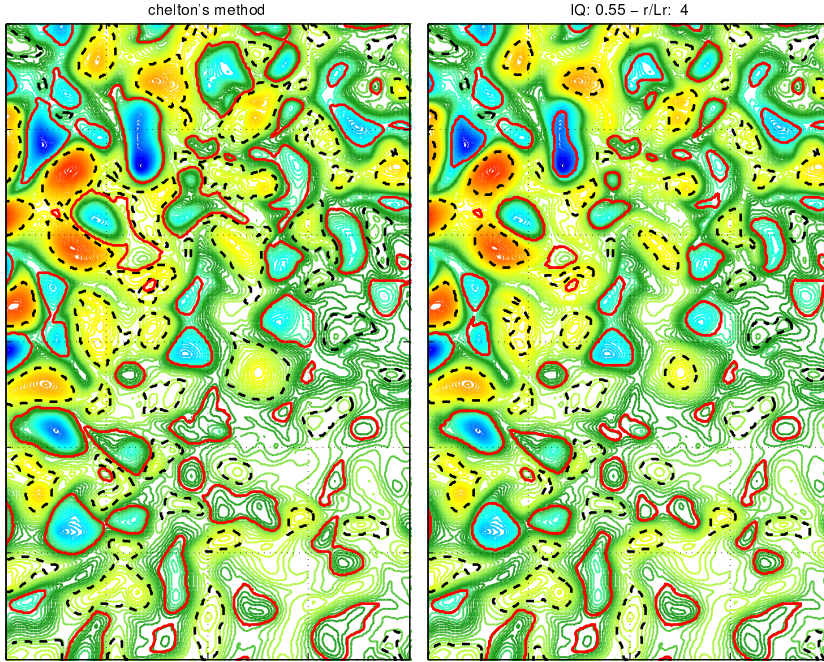


Figure 2.5: Left: The Chelton-method expects to detect eddies at their base and is rather tolerant with respect to the form of found contour. The IQ -method aims more at detecting single round vortices without expecting found contour to be necessarily related to any howsoever-defined outer *edge* of the eddy.

the absolute difference between SSH and current contour level and the position thereof as well as the amplitude relative to the mean SSH value of the eddy interior as done by [Chelton et al. \(2011\)](#). The amplitude is then tested against the user-given threshold. The function also creates a matrix with current contour level shifted to zero and all values outside of the eddy set to zero as well.

Contour filter 10 Chelton's Scales

```
function cheltStuff
Chelton et al. (2011) introduced 4 different eddy-scales.
```

1. The effective scale L_{eff} as the radius of a circle with its area equal to that enclosed by the contour.
2. The scale L_e as the radius at $z = e^{-1}a$ with a as the amplitude with reference to the original contour and the z -axis zero-shifted to that contour. In other words the effective scale of the contour that is calculated at $1/e$ of the original amplitude.
3. The scale $L = L_e/\sqrt{2}$.

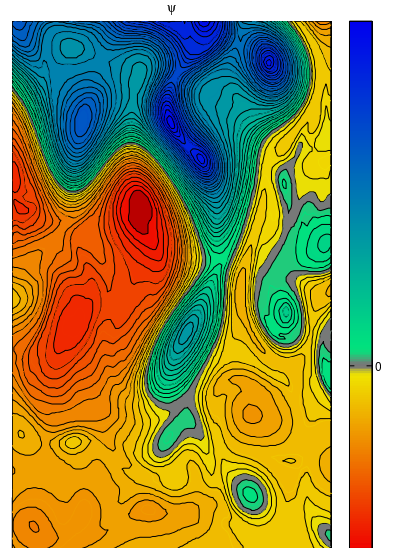


Figure 2.6: Stream function of a meandering jet shedding off a vortex. The line of strongest gradient *i.e.* fastest geostrophic speed later becomes the zero-vorticity-line at a theoretical distance σ from the center (Offset of Ψ is chosen arbitrarily).

4. The scale L_s which is *a direct estimate based on the contour of SSH within the eddy interior around which the average geostrophic speed is maximum* (Chelton *et al.*, 2011). It is hence conceptually the same as σ . This scale was not calculated here, as we could not think of an efficient, simple way to estimate the area bounded by maximum geostrophic speed *i.e.* the zero-vorticity contour. To understand why this would be difficult to achieve see also sections... **TODO:ref to approp sections eg noise in vort etc.**

Contour filter 11 Profiles

`function EddyProfiles`

This step

- saves the meridional and zonal profiles of SSH, U and V through the eddy's peak and spanning the entire sub-domain as described in 4.
- creates spline functions from the ssh-profiles and uses them to interpolate the profiles onto 100-piece equi-distant coordinate vectors to build smooth interpolated versions of ssh-profiles in both directions.
- in turn uses the splined data to create smooth 4-term Fourier-series functions for the profiles.

Contour filter 12 Dynamic Scale (σ)

`function EddyRadiusFromUV`

The contour line that is being used to detect the eddy is not necessarily a good measure of the eddy's *scale* *i.e.* it doesn't necessarily represent the eddy's outline very well. This becomes very obvious when the area, as inferred by 6, is plotted over time for an already successfully tracked eddy. The result is not a smooth curve at all. This is so because at different time steps the eddy usually gets detected at different contour levels. Since its surrounding continuously changes and since the eddy complies with the testing-criteria the better the closer the algorithm gets to the eddy's peak value, the determined area of the contour jumps considerably between time steps. This is especially so for large flat eddies with amplitudes on the order of 1cm. If the contour increment is on that scale as

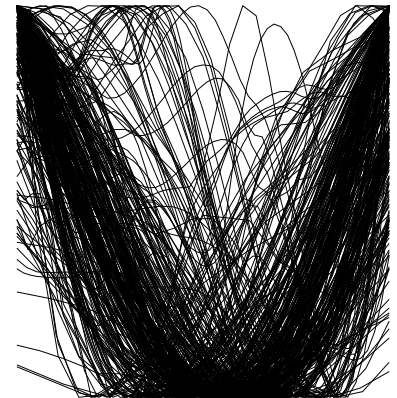


Figure 2.7: Zonal x- and z-normalized cyclone-profiles (early data ~ '13/12).

well, the difference in contour-area between two time steps easily surpasses 100% and more. Since there is no definition for the *edge* of an eddy, it is defined here as the ellipse resulting from the meridional (zonal) diameters that are the distances between the first local extrema of orbital velocity (one negative, one positive) away from the eddy's peak in y- (x-) directions ⁵. In the case of a meandering jet with a maximum flow speed at its center, that is shedding off an eddy, this scale corresponds to half the distance between two opposing center-points of the meander. It is also the distance at which a change in vorticity-polarity occurs and is thus assumed to be the most plausible dividing line between vortices.

Trying to determine the location where this sign change in vorticity occurs in the profiles turns out to be very tricky. What we seek are local extrema of the geostrophic speeds *i.e.* of the ssh-gradients h_x . In a perfect Gaussian-shaped eddy, these would simply correspond to the first local extrema of h_x away from the peak. In *reality* the eddies can be very wobbly with numerous local maxima and minima in the gradients of their flanks. One could argue, that it must be the largest extrema, as it is the highest geostrophic speeds that are sought. In practice ⁶ multiple superimposed signals of different scales often create very strong gradients locally. But the main issue here is that one weak eddy adjacent to one strong eddy also has the stronger gradients of the stronger one within its domain so that simply looking for the fastest flow speeds along the profiles is insufficient. It is also not possible to restrict the cut domain to the extent of a single eddy only, because at the point where the domain is selected, we do not know yet whether the detection algorithm *took bait* at the eddy's base or later close to the tip.

The best method thus far seems to be to use the Fourier-series functions from 11 to determine the first extrema away from the eddy's peak. The Fourier order was chosen to be 4 by trial and error. The effect is that small-scale low-amplitude noise is avoided, allowing for more reliable determinations of $\nabla^2 h_{\text{four}} = 0$

Once the zero crossings in all 4 directions are found, their mean is taken as the eddy's scale.

⁵The velocities are calculated from the gradients of 4th-order Fourier fits to the SSH profile in respective direction (see [TODO:ref](#)).

⁶especially for the high-resolution model data.

Contour filter 13 **Dynamic Amplitude**

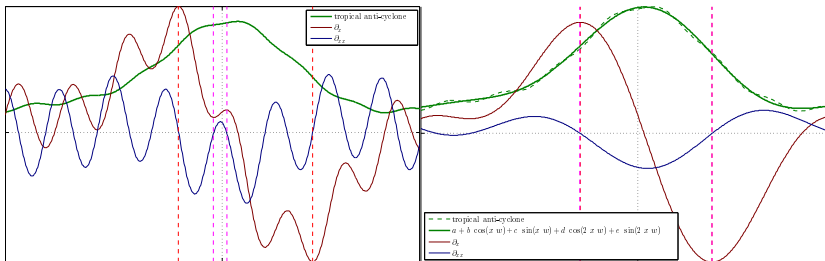


Figure 2.8: A flat wobbly low-latitude eddy resulting in multiple zero-crossings of its ∇^2 . The problem is addressed by differentiating the profile's Fourier-Series fit instead.

```
function EddyAmp2Ellipse
```

As mentioned above, the contour that helps to detect the eddy is not representative of its extent. This is also true for the z -direction, for the same reasons. This function therefore takes an SSH-mean at indices of the ellipse created by the determined zonal and meridional *dynamical* diameters, and uses this as the basal value to determine a *dynamic* amplitude.

Contour filter 14 Center of Volume (CoV)

```
function CenterOfVolume
```

Instead of using the geo-position of the eddy's peak in the tracking procedure, it was decided to instead use the center of the volume created by the basal shifted matrix from 9 *i.e. the center of volume of the dome (resp. valley) created by capping off the eddy at the contour level*. This method was chosen because from looking at animations of the tracking procedure it became apparent that, still using peaks as reference points, the eddy sometimes jumped considerably from one time step to the next if two local maxima existed within the eddy. E.g. in one time-step local maximum A might be just a little bit larger than local maximum B and one time-step later a slight shift of mass pushes local maximum B in pole position, creating a substantial jump in the eddy-identifying geo-position hence complicating the tracking procedure.

Contour filter 15 Geo Projection

```
function ProjectedLocations
```

An optional threshold on the distance an eddy is allowed to travel over one time-step is implemented in the tracking algorithm 2.5. This is a direct adaptation of the ellipse-based constraint described by Chelton *et al.* (2011). The maximum

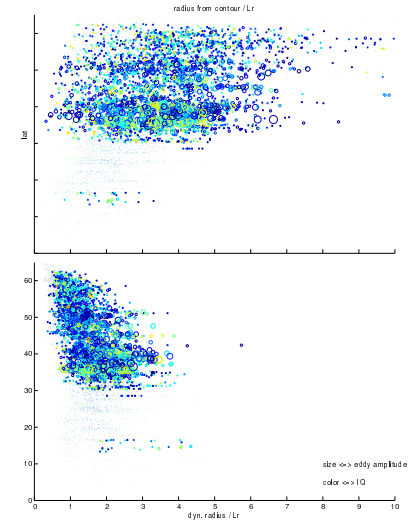


Figure 2.9: Eddies in the North-Atlantic. Y-axis: latitude. X-axis top: ratio of radius of circle with equal area to that of found contour to local Rossby-radius. X-axis bottom: ratio of σ to local Rossby-radius. Color-axis: Isoperimetric Quotient. Size: amplitude. The bottom plot suggests that a ratio of say 4 for σ/L_R should be a reasonable threshold. Same graph for the Southern Ocean looks very different though (not shown here), in that said ratio often exceeds ratios as high as 10 and larger in the far south where L_R becomes very small. This problem was addressed by prescribing a minimum value $L_R = 20\text{ km}$ for the calculation of the scale-threshold.

distance in western direction traveled by the eddy within one time-step is limited according to $x_{\text{west}} = \alpha c \delta t$ with c as the local long-Rossby-wave phase-speed and

e.g. $\alpha = 1.75$. In eastern direction the maximum is fixed to a value of *e.g.* $x_{\text{east}} = 150\text{km}$. This value is also used to put a lower bound on x_{west} and for half the minor axis (y -direction) of the resultant ellipse.

This function builds a mask of eligible geo-coordinates with respect to the next time-step.

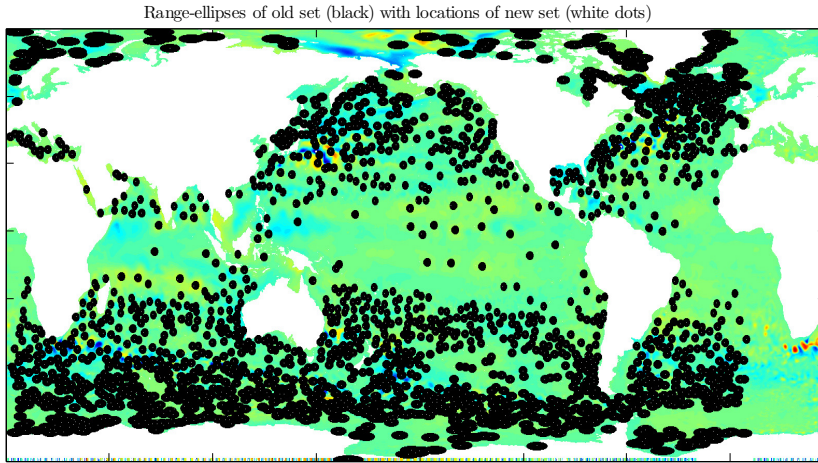


Figure 2.10: Among the saved meta-information for each eddy are also the indices describing the ellipse that defines the eddy's allowed locations with respect to the next time-step.

2.6 Step S05: Track Eddies

S05_track_eddies

2.6.1 Main Tracking Procedure

Due to the the relatively fine temporal resolution (daily) of the model data, the tracking procedure for this case turns out to be much simpler than the one described by [Chelton *et al.* \(2007\)](#). There is almost no need to project the new position of an eddy, as it generally does not travel further than its own scale in one day. This means that one eddy can usually ⁷ be tracked unambiguously from one time step to the next as long both time-steps agree on which eddy from the *other* time-step is located the least distance away. The algorithm therefor simply builds an arc-length-distance matrix between all old and all new eddies and then determines the minima of that matrix in both directions *i.e.* one array for the new with respect to the old, and one for the old with respect to the new set. This leads to the following possible situations:

- Old and new agree on a pair. *I.e.* old eddy O_a has a closest neighbour N_a in the new set and N_a agrees that O_a is the closest eddy from the old set. Hence the eddy is tracked. N_a is O_a at a later time.
- N_a claims O_a to be the closest, but N_b makes the same claim. *I.e.* two eddies from the new set claim one eddy from the old set to be the closest. In this situation the closer one is decided to be the old one at a later time-step and the other one must be a newly formed eddy.
- At this point all new eddies are either allocated to their respective old eddies or assumed to be *newly born*. The only eddies that have not been taken care of are those from the old set, that *lost* ambiguity claims to another old eddy, that was closer to the same claimed new eddy. *I.e.* there is no respective new eddy available which must mean that the eddy just *died*. In this case the entire track with all the information for each time step is archived as long as the track-length meets the threshold criterium. If it doesn't, the track is abandoned.

⁷The only exception being the situation when one eddy fades and another emerges simultaneously and in sufficient proximity.

2.6.2 Improvements

The former is the core of the tracking algorithm. It is almost sufficient by itself as long as the temporal resolution is fine enough. The larger the time-step, the more ambiguities arise, which are attempted to be mitigated by flagging elements of the distance matrix not meeting certain thresholds:

- `function checkDynamicIdentity`

Consider the ambiguous case when there are two eddies N_a and N_b in sufficient proximity to eddy O_a . Let's assume O_a is a relatively solid eddy of rel. large scale with a steep slope *i.e.* large amplitude and that N_a is merely a subtle blob of an eddy whilst N_b is somewhat similar to O_a but with only half the amplitude. The situation then is clear: N_b is the, apparently slowly dying, O_a at a later time, while N_a could either be a newly formed eddy, an old eddy with its respective representation in the old set something other than O_a , or even just temporary coincidental noise not representative of any significant meso-scale vortex. This interpretation should hold even when O_a sat right between the other two, thereby being much closer to O_a than N_b was.

The purpose of this step is to make such decisions. It does so by comparing the *dynamic* versions of amplitude and scale (*ampToEllipse* and σ) between the time-steps. If either ratio from new to old⁸ surpasses a given threshold the pair is flagged as non-eligible. It is important to use the *dynamic* parameters rather than those stemming from the contour line, because as mentioned in 12 the contour line itself and the eddy's geometric *character* are hardly correlated at all. One eddy can get detected at different z-levels from one time-step to the next, resulting in completely different amplitudes, scales and shapes with respect to the contour.

The initial idea was, by assuming Gaussian shapes, to construct a single dimensionless number representing an eddy's geometrical character built upon the contour-related amplitude- and scale values only. Since we have no information about the vertical position of a given contour with respect to assumed Gauss bell, this problem turned out to be intrinsically under-determined and hence useless. The method eventually used, which checks amplitude and scale

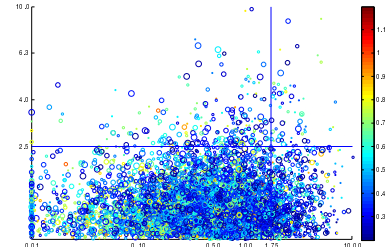


Figure 2.11: Each circle represents one eddy in the new time step. Y-axis: Maximum ratio to closest eddy in old set of either amplitude or σ , where 1 means *identical* and 2 means factor 2 difference. The threshold used for the final runs was 2. X-axis: Ratio of distance to closest eddy from old set divided by δt to local long-Rossby-wave phase-speed. Color-axis: Isoperimetric Quotient. Radius of circles: ratio of σ to local Rossby-radius. All eddies with said ratio larger than 10 are omitted. Note the obvious inverse correlation of scale to IQ, suggesting that all large eddies likely represent more than one vortex.

⁸ In order to compare in both directions equally: $\exp(|\log(v_n/v_o)|)$ where v is either amplitude or scale.

separately is again very similar to that described by [Chelton et al.](#) (see Box ??).

- `function nanOutOfBounds`

This is the second half to the prognostic procedure described in [2.6](#). It simply flags all pairs of the distance matrix for which the index representing the *new* eddy's geographic location is not among the set of indices describing the ellipse⁹ around respective *old* eddy.

⁹ see figure [2.10](#).

- `function checkAmpAreaBounds`

TODO:relevant only for chelton method!

2.7 Step S06: Cross Reference Old to New Indices

`function S05_init_output_maps`

The output Mercator-maps usually have different geometry from the input maps'. This step allocates all grid nodes of the input data to their respective nodes in the output map. Each output cell will then represent a mean (or median or std) of all input-nodes falling into that *square*.

2.7.1 Running the Code

The separate steps can be run all at once via `Sall.m` or one by one, as long as they are started consecutively in the order indicated by their name (`S00..`, then `S01..` ifnextchar.etcetc.). `S01b` is not necessary though. Each step saves its own files which are then read by the next step. All output data is saved in the user given root-path from [??](#). This concept uses quite a lot of disk space and is also quite substantially slowed by all the reading and writing procedures. The benefits, on the other hand, are that debugging becomes much easier. If the code fails at some step, at least all the calculations up to that step are dealt with and do not need to be re-run. The concept also makes it easy to extend the code by further add-ons.

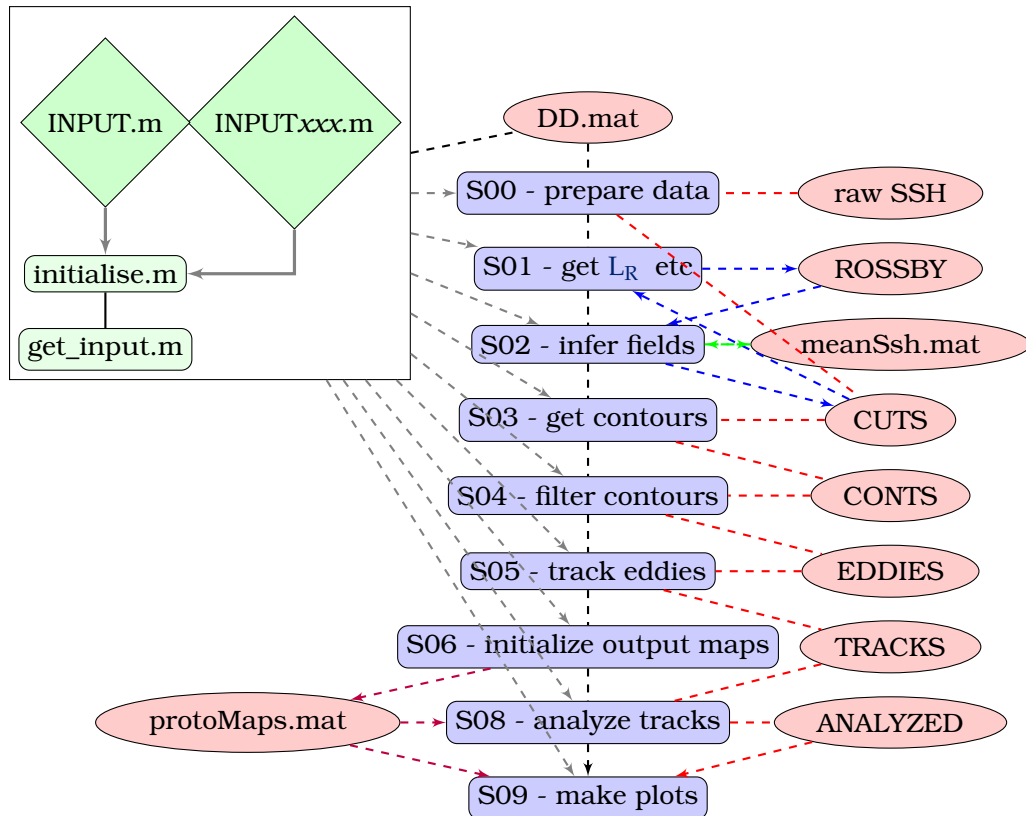


Figure 2.12: Basic code structure. The only files that are to be edited are the INPUT files. INPUT.m is independent of the origin of data, whilst the files INPUTTaviso.m, INPUTpop.m etc set source-specific parameters. Each of the SXX-steps initially calls initialise.m, which in turn scans all available data, reads in the INPUT data via get_input.m, corrects for missing data etc and creates DD.mat. The latter is the main meta-data file, which gets updated throughout all steps. All data is built step-by-step along the consecutive SXX-steps (red line). The SXX-steps are the only programs that have to be called (in order) by the user. Missing data is filled automatically in each step (Note that meanSsh.mat should be recalculated if the time span is changed!).

List of Figures

- 1.1 Animation snapshot of early test run. Shown is SSH with detected eddies indicated by red and green lines. 11
- 1.2 top: Stommel's equation $\mathcal{F}_{\text{bottom}} - \mathcal{F}_{\text{surface}} = -v\beta$ with constant eddy viscosity. bottom: Parallel Ocean Program eddy-resolving model snapshot with SSH mean of one year subtracted. 16
- 1.3 Resolutions for model vs satellite. Modified version from [Olbers et al. \(2012\)](#). 20
- 1.4 The ground track patterns for the 10-day repeat orbit of T/P and its successors Jason-1 and Jason-2 (thick lines) and the 35-day repeat orbit of ERS-1 and its successors ERS-2 and Envisat (thin lines). (a) The ground tracks of the 10-day orbit during a representative 7-day period; (b) The ground tracks of the 35-day orbit during the same representative 7-day period; (c) The combined ground tracks of the 10-day orbit and the 35-day orbit during the 7-day period; and (d) The combined ground tracks of the 10-day orbit and the 35-day orbit during the full 35 days of the 35-day orbit. (sic) [Chelton et al. \(2011\)](#) 21
- 1.5 Length of mission. Numbers are orbit-period in days. 21
- 1.6 $\xi(\phi, \mu)$. $Ny \equiv 2$ i.e. the Nyquist frequency. 21
- 2.1 SSH with mean over time subtracted. 25
- 2.2 **TODO:YO!** 27
- 2.3 Left: Fourier-fit of an eddy from POP-SSH-data and the 2nd differential thereof. Right: Theoretical Gauss-Shape built from the resulting *standard-deviation* i.e. σ and amplitude. 28
- 2.4 Different values of the isoperimetric quotient. 29

- 2.5 Left: The Chelton-method expects to detect eddies at their base and is rather tolerant with respect to the form of found contour. The IQ -method aims more at detecting single round vortices without expecting found contour to be necessarily related to any howsoever-defined outer *edge* of the eddy. 30
- 2.6 Stream function of a meandering jet shedding off a vortex. The line of strongest gradient *i.e.* fastest geostrophic speed later becomes the zero-vorticity-line at a theoretical distance σ from the center (Offset of Ψ is chosen arbitrarily). 30
- 2.7 Zonal x- and z-normalized cyclone-profiles (early data ~ '13/12). 31
- 2.8 A flat wobbly low-latitude eddy resulting in multiple zero-crossings of its ∇^2 . The problem is addressed by differentiating the profile's Fourier-Series fit instead. 33
- 2.9 Eddies in the North-Atlantic. Y-axis: latitude. X-axis top: ratio of *radius of circle with equal area to that of found contour* to local Rossby-radius. X-axis bottom: ratio of σ to local Rossby-radius. Color-axis: Isoperimetric Quotient. Size: amplitude. The bottom plot suggests that a ratio of say 4 for σ/L_R should be a reasonable threshold. Same graph for the Southern Ocean looks very different though (not shown here), in that said ratio often exceeds ratios as high as 10 and larger in the far south where L_R becomes very small. This problem was addressed by prescribing a minimum value $L_R = 20\text{km}$ for the calculation of the scale-theshold. 33
- 2.10 Among the saved meta-information for each eddy are also the indices describing the ellipse that defines the eddy's allowed locations with respect to the next time-step. 34
- 2.11 Each circle represents one eddy in the new time step. Y-axis: Maximum ratio to closest eddy in old set of either amplitude or σ , where 1 means *identical* and 2 means factor 2 difference. The threshold used for the final runs was 2. X-axis: Ratio of distance to closest eddy from old set divided by δt to local long-Rossby-wave phase-speed. Color-axis: Isoperimetric Quotient. Radius of circles: ratio of σ to local Rossby-radius. All eddies with said ratio larger than 10 are omitted. Note the obvious inverse correlation of scale to IQ, suggesting that all large *eddies* likely represent more than one vortex. 36

2.12Basic code structure. The only files that are to be edited are the INPUT files. INPUT.m is independant of the origin of data, whilst the files INPUTaviso.m, INPUTpop.m etc set source-specific parameters. Each of the SXX-steps initially calls initialise.m, which in turn scans all available data, reads in the INPUT data via get_input.m, corrects for missing data etc and creates DD.mat. The latter is the main meta-data file, which gets updated throughout all steps. All data is built step-by-step along the consecutive SXX-steps (red line). The SXX-steps are the only programs that have to be called (in order) by the user. Missing data is filled automatically in each step (Note that meanSsh.mat should be recalculated if the time span is changed!). 38

List of Tables

1.1 model vs satellite	20
------------------------	----

Bibliography

Bjerknes, J., & Holmboe, J. 1944. On the Theory of Cyclones. *J. Atmos. Sci.*

Chelton, Dudley B., Schlax, Michael G., Samelson, Roger M., & de Szoeke, Roland a. 2007. Global observations of large oceanic eddies. *Geophys. Res. Lett.*, **34**(15), L15606.

Chelton, Dudley B., Schlax, Michael G., & Samelson, Roger M. 2011. Global observations of nonlinear mesoscale eddies. *Prog. Oceanogr.*, **91**(2), 167–216.

Cipollini, Paolo, Cromwell, David, Jones, Matthew S, Quartly, Graham D, & Challenor, Peter G. 1997. Concurrent altimeter and infrared observations of Rossby wave propagation near 34°N in the Northeast Atlantic. *Geophys. Res. Lett.*, **24**(8), 889–892.

Cushman-Roisin, B. 1990. Westward motion of mesoscale eddies. *J. Phys.*

Eden, Carsten, & Greatbatch, Richard J. 2008. Towards a mesoscale eddy closure. *Ocean Model.*, **20**(3), 223–239.

Flierl, Glenn R. 1984. Rossby wave radiation from a strongly nonlinear warm eddy. *J. Phys. Oceanogr.*, **14**(1), 47–58.

Forget, Gaël. 2010. Mapping Ocean Observations in a Dynamical Framework: A 2004–06 Ocean Atlas. *J. Phys. Oceanogr.*, **40**(6), 1201–1221.

Killworth, Peter D., Chelton, Dudley B., & de Szoeke, Roland A. 1997. The Speed of Observed and Theoretical Long Extratropical Planetary Waves. *J. Phys. Oceanogr.*, **27**(9), 1946–1966.

- Le Traon, P-Y, & Minster, J-F. 1993. Sea level variability and semiannual Rossby waves in the South Atlantic subtropical gyre. *J. Geophys. Res. Ocean.*, **98**(C7), 12315–12326.
- Matano, Ricardo P, Schlax, Michael G, & Chelton, Dudley B. 1993. Seasonal variability in the southwestern Atlantic. *J. Geophys. Res. Ocean.*, **98**(C10), 18027–18035.
- Matsuura, Tomonori, & Yamagata, Toshio. 1982. On the evolution of nonlinear planetary eddies larger than the radius of deformation. *J. Phys. Oceanogr.*, **12**(5), 440–456.
- Nof, Doron. 1981. On the β -induced movement of isolated baroclinic eddies. *J. Phys. Oceanogr.*, **11**(12), 1662–1672.
- Oestreicher, Samantha. Underwater Mathematics : Illuminating Deep-Reaching Ocean Eddies in Climate Models.
- Okubo, Akira. 1970. Horizontal dispersion of floatable particles in the vicinity of velocity singularities such as convergences. *Deep sea Res. Oceanogr. Abstr.*, **17**(143), 445–454.
- Olbers, Dirk, Willebrand, Jürgen, & Eden, Carsten. 2012. *Ocean Dynamics*. Springer.
- Orbach, Michael K, & Munk, Walter. 2002. THE U . S . COM-MISSION ON OCEAN POLICY. *Natl. Acad. Sci. Washington, DC*, **15**(April), 135–141.
- Rhines, Peter B. 1974. Waves and turbulence on a beta-plane. *J. Fluid Mech.*, **69**(03), 417.
- Rhines, Peter B, & Holland, William R. 1979. A theoretical discussion of eddy-driven mean flows. *Dyn. Atmos. Ocean.*, **3**(2), 289–325.
- Smith, K. Shafer, & Marshall, John. 2009. Evidence for Enhanced Eddy Mixing at Middepth in the Southern Ocean. *J. Phys. Oceanogr.*, **39**(1), 50–69.
- van Leeuwen, Peter Jan. 2007. The Propagation Mechanism of a Vortex on the β Plane. *J. Phys. Oceanogr.*, **37**(9), 2316–2330.